

# Nucleation, Growth, Sintering, Mobility, and Adsorption Properties of Small Gold Particles on Polycrystalline Titania

E. Charles H. Sykes, Federico J. Williams, Mintcho S. Tikhov, and Richard M. Lambert\*

Chemistry Department, Cambridge University, Cambridge CB2 1EW, U.K.

Received: December 18, 2001

STM data show that gold exhibits homogeneous nucleation and growth on polycrystalline titania surfaces. When very small Au particles are exposed to ambient air at room-temperature rapid sintering occurs ( $\sim 20$  nm) accompanied by Au migration to titania crystallite grain boundaries. This process is driven principally by oxygen. Prolonged exposure to air induces further Au particle mobility resulting in agglomeration of the  $\sim 20$  nm particles at titania crystallite boundaries. It appears that water adsorption plays a role in this process. Work function measurements indicate that the very small Au clusters acquire a net positive charge and photoemission results reveal that their Au 4f BEs are increased relative to bulk gold. They also exhibit strongly enhanced adsorption and decomposition of styrene. This chemical effect is not a consequence of the charge state of the Au particles, rather it is a manifestation of a quantum size effect. The results are of significance to an understanding of the properties of Au/titania catalysts.

## Introduction

Highly dispersed Au particles supported on P25 titania exhibit unusual and unexpected catalytic behavior toward a number of important reactions including CO oxidation<sup>1,2</sup> and propene epoxidation<sup>3</sup>. Haruta et al.<sup>3</sup> have shown that these chemical effects are correlated with Au particle size, the interesting behavior generally occurring in the 2–4 nm range. Valden et al.<sup>4</sup> studied the corresponding model catalyst consisting of gold particles deposited on  $\text{TiO}_2$  {110}-(1  $\times$  1). They convincingly showed that 2–4 nm Au particles are characterized by an electronic structure different from that of bulk gold and do indeed exhibit enhanced catalytic activity toward CO oxidation. The origin of this extraordinary catalytic behavior is still a matter for debate and the issue has prompted a number of studies of the Au/titania system.<sup>4–8</sup> A characteristic and undesirable feature of the practical catalysts is their instability, a property whose cause is unclear.

Here we report the properties of 1–20 nm gold clusters supported on a polycrystalline titania surface grown in situ and consisting of  $\sim 60$  nm sized crystallites of  $\text{TiO}_2$ .<sup>9</sup> The intention was to generate systems that could serve as realistic model catalysts whose properties are closer to those of practical dispersed Au/P25–titania catalysts. The nucleation, growth, sintering, and agglomeration of Au clusters were monitored under realistic conditions of temperature and oxygen partial pressure. The chemisorption properties of styrene were also investigated. The latter has been proved useful in studies of terminal alkene epoxidation over  $\text{Ag}^{10}$  and Cu single-crystal surfaces<sup>11,12</sup> under UHV conditions; related to this, Au/titania catalysts exhibit high selectivity toward propene epoxidation.

## Experimental Methods

Experiments were performed in a VG ADES 400 electron spectrometer system operated at a base pressure of  $1 \times 10^{-10}$

Torr. The  $10 \times 10 \times 0.5$  mm<sup>3</sup> polycrystalline titanium sample (Advent, 99.6%) was secured to the xyz manipulator by spot welding to Ta strips. It could be resistively heated to 1350 K and cooled to 100 K. The principal impurities, sulfur, carbon, and phosphorus were removed by sputtering (15  $\mu\text{A}/5$  keV/900 K) with occasional flashes to 1300 K in order to segregate sulfur from the bulk. XP spectra were obtained with Mg  $K_{\alpha}$  radiation and UPS experiments were performed using a He I photon source. Gas exposure was carried out with a tube doser to enhance the flux at the sample position. Styrene (Aldrich, 99%) and de-ionized water were purified by repeated freeze/pump/thaw cycles and Messer grade 4.8 oxygen was used for the oxidation procedures. Gas purities were monitored by mass spectrometry and quoted exposures are in Langmuirs (1 L =  $10^{-6}$  Torr s<sup>-1</sup>), uncorrected for ion gauge sensitivity. The polycrystalline titania films were grown in situ by controlled oxidation of a cleaned polycrystalline titanium sample. Their preparation and morphological and chemical characterization have been described in detail elsewhere.<sup>9,13</sup> The procedure employed resulted in a titania film whose  $\text{Ti}^{3+}$  surface concentration was below the detection limit of XPS. Gold was deposited by means of a collimated evaporation source. Evaporation rates were typically 0.1 ML/min at background pressures  $< 5 \times 10^{-10}$  Torr. The Au deposition rate was calibrated by depositing gold on titanium *metal* (Frank–van der Merwe growth) while monitoring the Ti 2p and Au 4f relative intensities. Therefore on the titania surfaces gold loadings are given in equivalent monolayers (ML). After sample preparation in UHV, ex-situ STM data were acquired under ambient laboratory conditions using a Zeiss-Beetle SPM operating in the STM mode using chemically etched W tips. The UHV-STM data were taken using an Omicron VT-STM-1 instrument using similar tips. This apparatus included a preparation chamber and fast entry lock that were used to expose the sample to both pure oxygen and air at atmospheric pressure. The Au cluster diameters quoted correspond to raw data taken from the STM images. They are uncorrected for finite tip size effects and are therefore upper limits. For TPD/TPR measurement (15 K/s) the

\* Corresponding author. Fax: + 44 1223 336362. E-mail: RML1@cam.ac.uk.

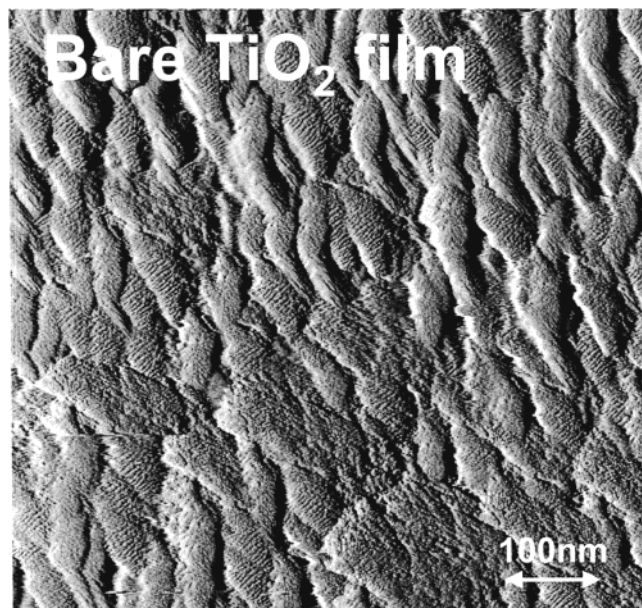


**Figure 1.** Ex-situ STM image ( $630 \times 630$  nm/ $V_{\text{tip}} = +0.7$  V/ $I = 0.4$  nA) showing nano-crystallites of titania film prepared by oxidizing polycrystalline titanium metal.

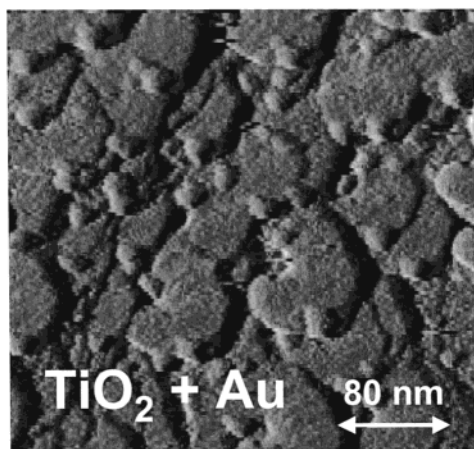


**Figure 2.** Ex-situ STM image ( $320 \times 320$  nm/ $V_{\text{tip}} = +0.7$  V/ $I = 0.4$  nA) showing nucleation of 3 equiv. ML gold at the edges of the titania nano-crystallites.

sample was positioned 2 cm from the collimated quadrupole mass spectrometer (QMS) ionizer so that the signal arose almost entirely from the front face. Work function measurements were made by the He I low energy cutoff method, following established procedures whereby sample biasing was employed to improve the sharpness of the cutoff.<sup>14</sup> Based on observation of the Fermi edge of the Ti films before oxidation, the estimated instrumental resolution was 0.03 eV. The run-to-run reproducibility of Df measurements was  $\pm 0.1$  eV, but the precision within a run was  $\pm 0.02$  eV.

## Results and Discussion

**Ex-Situ STM Results: Nucleation, Growth, Sintering, and Agglomeration of 20 nm Gold Clusters on Polycrystalline  $\text{TiO}_2$ .** The sequence of STM images presented in Figures 1, 2, and 3 shows, respectively, the bare  $\text{TiO}_2$  surface, the same surface immediately after Au deposition, and then after prolonged exposure to air. Figure 1 shows the as-prepared  $\text{TiO}_2$  film which exhibited crystallites of average diameter 60 nm. These grew in a variety of shapes. Thus the  $\text{TiO}_2$  crystallites in

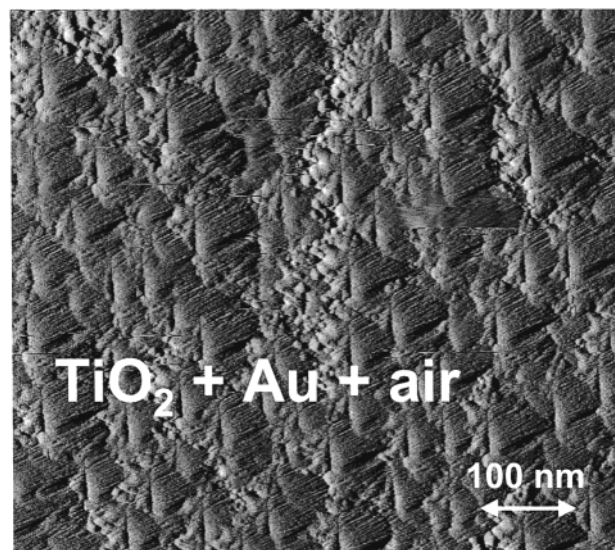


**Figure 3.** Ex-situ STM image ( $630 \times 630$  nm/ $V_{\text{tip}} = +0.7$  V/ $I = 0.4$  nA) showing agglomeration of 3 equiv. ML gold after exposure to lab air prior to 200 h stored in desiccator.

Figure 1 resemble elongated ovals, those in Figure 2 have “kidney bean” shapes, while Figure 3 shows triangular crystallites. These variations in morphology are thought to reflect morphological variations in the underlying Ti metal upon which the oxide film was grown, probably due to variations in heating and cooling rates during initial cleaning and annealing procedures. Gold deposition led to metal cluster nucleation at the edges of the titania crystallites. Figure 2 shows the result of depositing 3 ML gold under UHV conditions before sample transfer to the ex-situ STM. This image shows Au clusters representative of the whole sample with a mean diameter of  $\sim 20$  nm and with a truncated hemispherical shape. Au nucleation at titania crystallite edges is at least consistent with the findings of Goodman and co-workers<sup>4</sup> who reported that gold sintering is suppressed on a rough  $\text{TiO}_2$  {110} surface as compared to the corresponding smooth surface. A possible implication is that Au binds preferentially to low coordination sites on the oxide surface. However, this does not necessarily mean that Au nucleation occurs preferentially at crystallite boundaries, as we shall see below. It was observed that exposure of these samples to laboratory air for a number of days resulted in agglomeration of the Au clusters at the titania crystallite boundaries. The image shown in Figure 3 is from a sample that had been exposed to laboratory air for 24 h, followed by 200 h in a vacuum desiccator. It is apparent that the  $\sim 20$  nm Au clusters have agglomerated at the titania crystallite edges. We conclude that either water or oxygen adsorption at room temperature are responsible for redistribution of the gold clusters, an issue that is pursued further in the next section.

**In-Situ UHV-STM Results: Nucleation, Morphology, and Sintering of 2–4 nm Gold Clusters.** To investigate certain aspects of the system in more detail, experiments were carried out in which titania growth, Au particle deposition, and subsequent examination were performed in the same UHV apparatus. This methodology also enabled us to study very small gold clusters whose size lies in the range relevant to the appearance of interesting catalytic properties.<sup>3,4</sup> Having demonstrated that either oxygen or water can induce cluster mobility, we studied the effects of both pure oxygen and laboratory air in a controlled manner by means of the sample transfer/environmental cell facility. Figure 4 shows a representative image taken from a freshly prepared sample (0.5 ML Au/ $\text{TiO}_2$ )



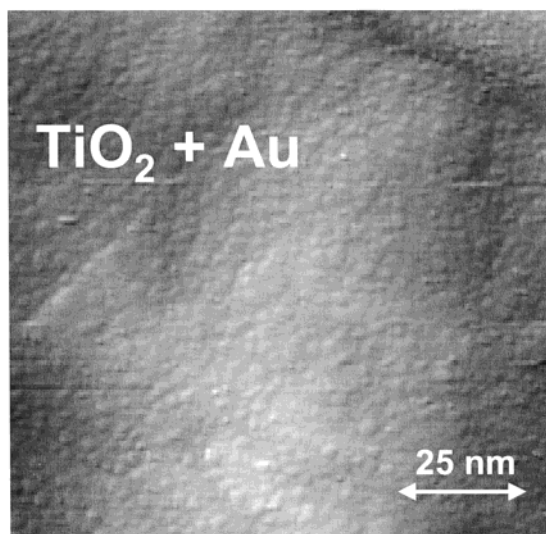


**Figure 4.** UHV-STM image ( $100 \times 100$  nm/ $V_{\text{tip}} = +1$  V/ $I = 1$  nA) showing 0.5 equiv. ML gold freshly deposited.

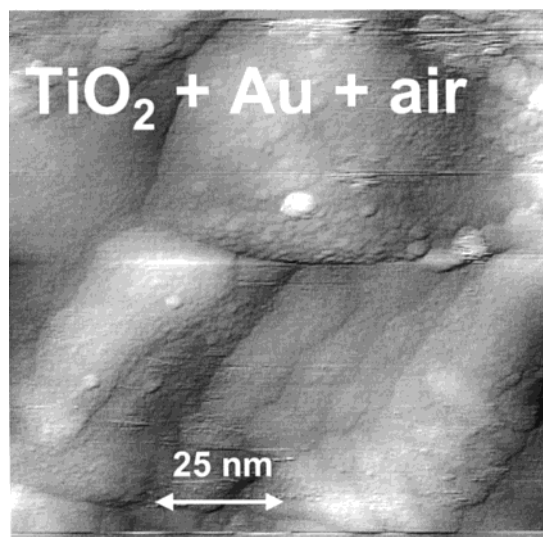


**Figure 5.** UHV-STM image ( $100 \times 100$  nm/ $V_{\text{tip}} = +1$  V/ $I = 1$  nA) showing 0.5 equiv. ML gold after exposure to 1 bar  $\text{O}_2$ /18 h at 300 K.

characterized by a mean Au cluster size of 2.5 nm. Interestingly, in this image the Au cluster sizes and nucleation patterns are very similar to those measured by Valden et al.<sup>4</sup> for Au clusters on a single-crystal surface of  $\text{TiO}_2$ . Note that the Au particles are uniformly distributed and show no particular tendency to decorate titania crystallite boundaries. This is an important result. It shows that in the case of the *ex situ* STM work discussed in the previous section, where samples were prepared in an identical fashion, the results shown in Figure 2 are *not* a consequence of Au nucleation at titania crystallite boundaries. The actual sequence of events must have been as follows: (1) initial deposition of Au resulted in a uniform distribution of Au clusters, (2) upon exposure to air, individual clusters migrated to neighboring titania grain boundaries (Figure 2), and (3) longer exposure to air resulted in agglomeration of the Au clusters at the grain boundaries (Figure 3).

Let us return to the sample imaged in Figure 4. Exposure of this to 1 bar of pure oxygen for 18 h at room temperature resulted in pronounced sintering of the Au clusters, as illustrated in Figure 5. After sintering, the mean gold particle diameter was 4 nm with some clusters as large as 9 nm being observed. The quoted Au cluster dimensions before and after oxygen

treatment are mean values calculated from cluster size distributions measured at several points on the sample. Due to the inhomogeneity of the sample and the relatively small number of clusters measured it is not possible to determine the mode of cluster growth. However, it is certainly clear that growth occurred, oxygen treatment has increasing the mean diameter from 2.5 to 4 nm. From Figure 5 it is apparent that the larger clusters were not located at grain boundaries: the conclusion is that the main effect of oxygen was to induce Au particle growth as opposed to migration of Au clusters to titania grain boundaries. Similar experiments (not illustrated) were performed in which the sample was exposed to laboratory air at atmospheric pressure for 18 h at room temperature. The resulting sintering was essentially the same as in pure oxygen, suggesting that  $\text{O}_2$  is principally responsible for the facile room-temperature sintering of gold clusters on  $\text{TiO}_2$ .

This behavior is related to that reported by Goodman et al.<sup>8</sup> who found that at 450 K on  $\text{TiO}_2\{110\}$  Au clusters  $< 4$  nm in diameter were unstable with respect to sintering in the presence of  $> 10^{-1}$  Torr oxygen. They offered the following plausible explanation. Because very small Au clusters are effective oxidation catalysts they must be capable of absorbing oxygen. This could weaken the Au–Au bonds in the cluster, thus promoting sintering. Given their results and ours, the following conclusions appear to be justified. First, nanoscopic Au particles on  $\text{TiO}_2$  are readily sintered under very mild oxidizing conditions—low oxygen pressures and modest temperatures or high oxygen pressure and room temperature. Second, this behavior appears to be insensitive to the details of the titania surface structure: it is unlikely that the surfaces of all our 60 nm  $\text{TiO}_2$  crystallites were dominated by extended areas consisting of  $\{110\}$  planes. (A corollary of the second conclusion is that studies on  $\text{TiO}_2\{110\}$  are indeed pertinent to an understanding of the properties of titania-supported metal catalysts).

There are two effects to be understood: the growth of small Au particles and migration of  $\sim 20$  nm Au particles to titania grain boundaries. The first effect may be understood in terms of the mechanism proposed by Kolmakov et al.<sup>8</sup> which involves the effect of oxygen adsorption on small Au particles. However we may postulate an alternative mechanism based on the effect of oxygen on the titania component, as follows. Upon initial deposition of Au oxygen vacancies are created at the Au/titania interface.<sup>15</sup> These vacancies induce a strong interaction between the metal and oxide phases, contributing to the adhesion between the two. Subsequent exposure to oxygen leads to filling of these vacancies at a rate that depends on temperature and oxygen pressure. The result is an increased mobility of Au, either by particle migration as observed by Mitchell et al.<sup>16</sup> in the case of very small particles or by Ostwald ripening in the case of larger particles (the proposed mechanism implies a lowering of the activation energy for detaching Au atoms from particle boundaries).

Further work is required to decide between the two possibilities discussed above. However, neither hypothesis accounts for the pronounced tendency of relatively large ( $\sim 20$  nm) Au particles to agglomerate at grain boundaries upon exposure to air. Our earlier work<sup>9,13</sup> shows that water desorbs from these titania films at  $\sim 340$  K. Therefore the air-exposed Au/titania samples must inevitably have fully hydrated surfaces that may promote Au particle mobility, leading to their accumulation at titania grain boundaries. Mobility of 2.5 nm Au clusters on  $\text{TiO}_2\{110\}$  at  $\sim 750$  K in UHV has been observed;<sup>16</sup> in the light of this, water-assisted migration of  $\sim 20$  nm particles under ambient conditions seems not implausible. Whatever the mech-

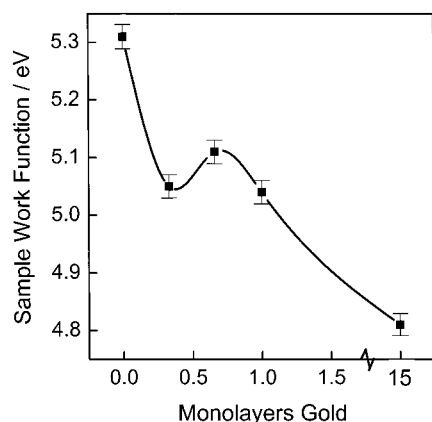


**Figure 6.** Variation of sample work function with increasing gold coverage.

anism, it seems at least possible that the facile sintering and agglomeration behavior found here on polycrystalline titania underlies the instability of dispersed Au/titania catalysts.

**Electronic Structure of Small Gold Particles.** Earlier results obtained with gold clusters supported on various oxides<sup>5,17,18</sup> have been interpreted in terms of electrostatic charging of the metal as a result of interaction with the oxide. For example, in their XPS work on  $\text{TiO}_2\{110\}/\text{Au}$ , Zhang et al.<sup>5</sup> interpreted the observed Au 4f BE shift in terms of reduced core hole screening in the final state, although they did not rule out absolutely the possibility that the Au had acquired a net positive charge in the initial state. The question of the extent and polarity of charge transfer between small metal particles and oxides such as  $\text{TiO}_2$  has been considered by several authors. A rigorous, comprehensive, and quantitative examination of the issue within the context of Schottky junction formation has been carried out by Ionnides and Verykios.<sup>19</sup> The same issue arises here, specifically in regard to effects on the adsorption of styrene, and we address it by a combination of  $\Delta\phi$  and XPS measurements.

**Work Function Measurements.** By measuring the low energy cutoff in the UP spectra one may measure changes in sample work function; knowing the energy of the incident photons, the absolute work function may be deduced. Note that for inhomogeneous "patchy" samples such as ours, this method of measurement gives average values that correspond to the area-weighted work function.<sup>20,21</sup> Thus as gold is progressively added to the titania surface a smooth variation in  $\phi$  with Au loading would be expected between  $\phi(\text{TiO}_2) = 5.3 \text{ V}$ <sup>22</sup> and  $\phi(\text{Au}) = 5.0 \text{ V}$ .<sup>23</sup> If the Au area increased linearly with Au loading (which it does not) the dependence should be linear. Figure 6 shows the results of such an experiment. The clean  $\text{TiO}_2$  surface had a work function of 5.3 V, in excellent agreement with the literature value of 5.3 V.<sup>22</sup> At the highest gold loading the work function was 4.8 V, in good agreement with the literature value for polycrystalline gold.<sup>23</sup> The variation between these two limits is fairly smooth, except that at 0.3 ML Au a clear local minimum appears. A possible interpretation of Figure 6 is that for loadings  $\leq 0.5 \text{ ML}$ , where the Au cluster size is  $\sim 2.5 \text{ nm}$  or less, the gold particles are positively charged with respect to the  $\text{TiO}_2$  and the associated dipole results in a lowering of the local  $\phi$ . Given that the work function of Au is substantially less than that of fully stoichiometric procedure, Schottky junction formation could in principle lead to  $\text{Au} \rightarrow \text{TiO}_2$  electron transfer.<sup>19</sup>

**Initial and Final State Effects on Au 4f Binding Energy.** Figure 7 shows Au 4f spectra as a function of increasing gold loading. A shift to higher binding energy is observed for coverages  $\leq 2 \text{ ML}$ . For example, at 1 ML Au ( $\sim 2 \text{ nm}$ ) the Au

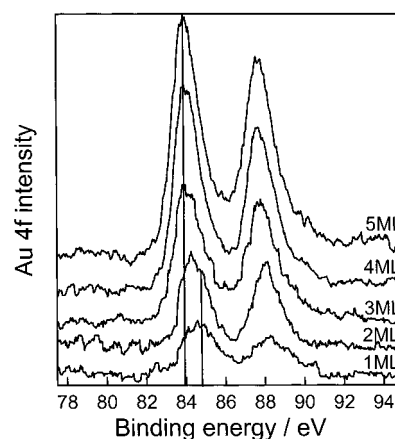


**Figure 7.** XPS, Au 4f of increasing coverages of gold on  $\text{TiO}_2$ .

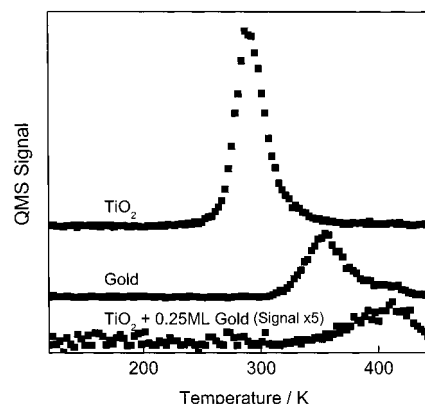


**Figure 8.** TPD of 0.02 ML styrene on titania, gold, and titania/0.25 ML gold surfaces.

4f<sub>7/2</sub> core level BE is 0.6 eV higher than that of bulk gold. Given the above  $\Delta\phi$  data that suggest positive charging of very small gold particles, these shifts in the Au 4f level could contain an initial state contribution due to the positive charging of Au, in addition to a final state effect associated with reduced core hole screening.<sup>5</sup> For a sufficiently small Au particle, electronic charge depletion could conceivably affect its chemical properties: we now consider the adsorption behavior of styrene as a function of Au particle size.

**Desorption of Styrene from Titania and Gold/Titania Surfaces.** Figure 8 shows temperature-programmed desorption data obtained after dosing 0.01 L styrene at 130 K (equivalent to 0.02 ML coverage) onto (i) clean  $\text{TiO}_2$ , (ii)  $\text{TiO}_2/30 \text{ ML Au}$  (effectively a pure gold surface), and (iii)  $\text{TiO}_2/0.25 \text{ ML Au}$  ( $\sim 2 \text{ nm}$  gold). Desorption from pure  $\text{TiO}_2$  occurs in a peak centered at 290 K, whereas desorption for the gold surface a broader peak centered at 350 K is found. It is apparent that desorption fingerprint of the  $\sim 2 \text{ nm}$  Au/titania sample does not correspond to a superposition of those of the pure components. In this case the desorption peak temperature is highest of all (410 K) and the desorption yield is strongly reduced. These results were repeatedly reproducible clearly demonstrating the chemical effects of the presence of very small Au particles. The reduced styrene yield and higher desorption temperature are consistent with stronger binding and extensive decomposition of the adsorbate on the very small Au particles. Note also that on this sparsely covered titania surface, no desorption characteristic of titania sites is observed. The implication is that at temperatures  $\leq 250 \text{ K}$  titania-adsorbed styrene molecules become mobile, diffuse to the Au particles where they are

strongly held, subsequently decomposing/desorbing at higher temperatures.

What is the cause of enhanced styrene binding to very small Au particles? If the particles were positively charged, as they appear to be, the associated valence electron depletion would be expected to enhance binding of  $\pi$ -donors such as styrene. However, a crude estimate based on classical electrostatics enables us to rule out this possibility. Thus even if we ascribe the entire Au 4f BE shift of the  $\sim 2$  nm particles to charging in the initial state, the associated charge transfer corresponds to  $\sim 0.003$  electrons /Au atom. We are left with the possibility that the enhanced binding of styrene to nanoscopic Au is a manifestation of a quantum size effect that is also responsible for unusual catalytic properties of very small gold particles.

## Conclusions

1. Gold exhibits homogeneous nucleation and growth on polycrystalline titania surfaces.

2. Exposure of very small Au particles to ambient air at room temperature causes rapid sintering and migration to titania crystallite grain boundaries. This sintering is principally an effect of oxygen. Prolonged exposure to air induces further Au particle mobility leading to agglomeration of the particles at titania crystallite boundaries. It appears that water adsorption plays a role in this process.

3. The very small Au clusters ( $< 2.5$  nm) acquire a net positive charge and exhibit higher Au 4f BEs relative to bulk gold. They also exhibit strongly enhanced adsorption of styrene. This chemical effect is not a consequence of the charge state of the Au particles. It is a manifestation of a quantum size effect.

**Acknowledgment.** Financial support from the U.K. Engineering and Physical Sciences Research Council under Grant GR/M76706 is gratefully acknowledged. E.C.H.S. acknowledges

the award of an EPSRC research studentship and additional support from the Newton Trust.

## References and Notes

- (1) Bollinger, M. A.; Vannice, M. A. *App. Catal. B* **1996**, 8, 417.
- (2) Grunwaldt, J. D.; Kiener, C.; Wogerbauer, C.; Baiker, A. *J. Catal.* **1999**, 181, 223.
- (3) Hayashi, T.; Tanaka, K.; Haruta, M. *J. Catal.* **1998**, 178, 566.
- (4) Valden, M.; Lai, X.; Goodman, D. W. *Science* **1998**, 281, 1647.
- (5) Zhang, L.; Persaud, R.; Madey, T. E. *Phys. Rev. B* **1997**, 56, 549.
- (6) Zhang, L.; Cosandey, F.; Persaud, R.; Madey, T. E. *Surf. Sci.* **1999**, 439, 73.
- (7) Lai, X.; St. Clair, T. P.; Valden, M.; Goodman, D. W. *Prog. Surf. Sci.* **1998**, 59, 25.
- (8) Kolmakov, A.; Goodman, D. W. *Catal. Lett.* **2000**, 70, 93.
- (9) Sykes, E. C. H.; Tikhov, M. S.; Lambert, R. M. *J. Phys. Chem. B*, submitted.
- (10) Hawker, S.; Mukoid, C.; Badyal, J. P. S.; Lambert, R. M. *Surf. Sci.* **1989**, 219, L615.
- (11) Cowell, J. J.; Santra, A. K.; Lindsay, R.; Lambert, R. M.; Baraldi, A.; Goldoni, A. *Surf. Sci.* **1999**, 437, 1.
- (12) Santra, A. K.; Cowell, J. J.; Lambert, R. M. *Catal. Lett.* **2000**, 67, 87.
- (13) Sykes, E. C. H.; Tikhov, M. S.; Lambert, R. M. *Catal. Lett.*, submitted.
- (14) Holzl, J.; Schulte, F. K. *Springer Tracts in Modern Physics*; Holzhler, G., Ed.; Springer-Verlag: Berlin, 1979; Vol. 85, Chapter 1.
- (15) Frost, J. C. *Nature* **1988**, 334, 577.
- (16) Mitchell, C. E. J.; Howard, A.; Carney, M.; Egdell, R. G. *Surf. Sci.* **2001**, 490, 196.
- (17) Sanchez, S.; Abbet, S.; Heiz, U.; Schneider, W. D.; Hakkinen, H.; Barnett, R. N.; Landman, U. *J. Phys. Chem. A* **1999**, 103, 9573.
- (18) Boccuzzi, F.; Chiorino, A.; Manzoli, M. *Surf. Sci.* **2000**, 454–456, 942.
- (19) Ionnides, T.; Verykios, X. E. *J. Catal.* **1996**, 161, 560.
- (20) Fischer, S.; Schierbaum, K.-D.; Gopel, W. *Sensors Actuators B* **1996**, 31, 13.
- (21) Schierbaum, K.-D.; Fischer, S.; Torquemada, M. C.; de Segovia, J. L.; Roman, E.; Martin-Gago, J. A. *Surf. Sci.* **1996**, 345, 261.
- (22) Onishi, H.; Aruga, T.; Egawa, C.; Iwasawa, Y. **1990**, 233, 261.
- (23) Ibach H.; Luth, H. *Solid State Physics*; Springer-Verlag: Berlin, 1990; p 101.